



Effect of pre-weld tempers on mechanical and microstructural behavior of dissimilar friction stir welds of AA2014 and AA7075

Raj Kumar^{a*}, Vikas Upadhyay^a, & Chaitanya Sharma^b

^aDepartment of Mechanical Engineering, National Institute of Technology Patna, Patna 800 005, India

^bDepartment of Mechanical Engineering, Birsa Institute of Technology Sindri, Dhanbad 828 123, India

Received: 6 February 2021; Accepted: 1 September 2021

In this work, friction stir welding of AA2014 and AA7075 has been performed in different combinations of T6 and O temper to study the influence of base metal temper on microstructure, mechanical properties, and fracture behavior of developed welds. Four dissimilar welded joints have been developed using optimum process parameters: AA2014-T6 with AA7075-T6, AA2014-O with AA7075-T6, AA2014-T6 with AA7075-O, and AA2014-O with AA7075-O. The stir zone microstructure has been dominated by the base metal placed on the advancing side and has equiaxed grains without constituent particles. Weld joints' strength has been either nearly equal or higher than that of low strength base metal, whereas the weld failure has taken place from the base metal region when at least one base metal was in O temper and from Stir Zone (SZ) when base metal was in T6 temper.

Keywords: Friction Stir Welding, Dissimilar aluminum alloys, Pre-weld Temper, Mechanical properties, Microstructure

1 Introduction

Among various aluminum alloys, AA2xxx and AA7xxx series alloys are high-strength heat-treatable alloys that have been widely used in various aerospace applications. AA2014 and AA7075 are aerospace alloys that are also readily used in the marine and automotive industries because of their inherent properties of high strength and low specific weight^{1,2}. The strength of AA7075 is higher than the strength of the structural steel³. AA7075 is a quaternary alloy comprising Al-Zn-Cu-Mg, while AA2014 is a ternary alloy comprising Al-Cu-Mg. The main alloying element Cu is responsible for the poor weldability of these alloys when welded by fusion welding processes⁴. However, these aluminum alloys are readily weldable by solid-state friction stir welding (FSW)⁵.

FSW is a hot working process that joins members by plastic deformation and material flow in the solid state at recrystallization temperature below the melting point of base metal (BM)⁶. Thus, FSW eliminates problems and defects related to fusion welding of aluminum alloys like solidification and liquation cracking, porosity, loss of an alloying element, softening⁷. Along with various factors such as input parameters, tool geometry, tool offset, in-

process cooling, to name a few, the pre-weld temper of the base material also significantly affects the weld properties. T3, T4, and T6 have been the most commonly used BM temper conditions⁸. Annealed O temper condition of aluminum alloy has been used where the formability is the foremost requirement². The literature on pre-weld tempers' effect on similar and dissimilar friction stir welds of heat treatable aluminum alloys is briefly reviewed below.

Pre-weld tempers significantly affect the microstructural and mechanical properties of the friction stir welded joints^{9, 10}. Chen *et al.*, 2006 have studied the effect of O and T6 temper of AA2219 alloy and reported 100% strength efficiency for AA2219-O and 82% for AA2219-T6. O temper joints fractured from advancing side (AS) whereas T6 temper joints fractured from retreating side (RS). Maximum tensile properties were obtained with T6 pre-weld temper in FSW joints of AA2024, whereas AA2024-O joints were stronger than BM¹¹. Yan *et al.*¹² have reported that FSW of AA7050 in W temper followed by post-weld ageing provides improved ultimate tensile strength (UTS), yield strength (YS), and percentage elongation (PE) as compared to welding in T62 and T7451.

AA7075-O welded joints have strength higher than BM, whereas AA7075-T6 welded joints' strength lower than their BM. The former is strengthened by

*Corresponding author (E-mail: rajk.phd15.me@nitp.ac.in)

solid solution only, while T6 joint strengthening is caused by coarsening and dissolution of strengthening precipitates¹³. In friction stir welds of AA7039 fabricated in O, W, and T6 temper conditions, the weld nugget was softer in T6 and W temper welds than their respective BMs, while reverse results were observed for O temper welds. Fracture location was also affected by a change in temper condition of BMs¹⁰. FSW of AA 7055 in T6 and T4 temper has been performed by Lin *et al.*¹⁴ and reported higher UTS, YS, and PE in T4 joints than in T6 joints. The SZ hardness of T6 joints was also observed slightly lower than the T4 joints. In friction stir welds of anSc-modified Al-Zn-Mg alloy in hot rolled and T6 temper, the weld efficiency of hot rolled alloy joints was more than 90%, whereas 70% in T6 alloy joints¹⁵. Effect of annealed, and age hardened pre-weld temper conditions on the performance of FSW joints of Al-4 wt.% Cu alloys have been studied by Al-Dwairi *et al.*¹⁶. They reported that the age-hardened pre-weld temper resulted in higher hardness, penetration, and wear resistance in joint zones than the annealed one.

Dissimilar FSW of AA7075-O and AA2024-T4 has been performed by Bahemmat *et al.*² keeping in view the formation limitation of AA 7075-T6. Friction stir welding of AA7075 and AA6061 in O and T6 temper has been performed by Ipekoglu and Cam¹⁷ and observed an increase in hardness in SZ when welded in O temper and vice versa. Irrespective of the initial temper, all the joints failed from low strength BM AA6061, and the microstructure of SZs was inhomogeneous, comprising both the alloys.

Much work has been reported on the effect of the pre-weld temper of similar FSW joints. Still, very few papers have been reported on the effect of pre-weld temper on dissimilar FSW of AA2xxx and 7xxx series. That too was with similar T6 or O temper, i.e., either both BMs are in O-O or T6-T6 temper. Therefore, it is required to explore this area further and investigate the effect of the dissimilar welds with dissimilar pre-weld tempers of aluminum alloy in O and T6 tempered conditions, i.e., O-T6 or T6-O. Thus, the present work studies the effect of pre-weld temper conditions on dissimilar friction stir welded joints of AA2014 and AA7075

with various combinations of O and T6, i.e., similar and dissimilar temper.

2 Materials and Methods

2.1 Chemical composition and mechanical properties

The chemical composition and mechanical properties of AA2014 and AA7075 are presented in Table 1 and Table 2.

2.2 Pre-weld heat treatment

Pre-weld heat treatments were performed on as-received base materials to change their temper from peak hardened T6 to annealed O. The 6 mm thick plates of AA2014 and AA7075 were machined to a size of 140 mm × 50 mm. AA2014-T6 plates were heated to the solutionizing temperature of 415°C, soaked for 2 hours, and then the furnace cooled to 260°C at 30 °C/h. Plates of AA7075-T6 were heated to 415°C, soaked for 2 hours, cooled to 205 °C, then reheated to 230 °C for 4hour¹⁸. To investigate the influence of pre-weld heat treatment, i.e., temper condition of BMs, dissimilar friction stir weld joints using optimum process parameters were developed in the following combinations.

(i) 2T6-7T6 (AA2014-T6 with AA7075-T6), (ii) 2O-7T6 (AA2014-O with AA7075-T6), (iii) 2T6-7O (AA2014-T6 with AA7075-O), and (iv) 2O-7O (AA2014-O with AA7075-O).

2.3 Machine and tool details

The FSW was performed on a numeric controlled (NC) vertical milling machine (Make: Manford; Model: VL 760) in butt joint configuration using an optimum rotational speed of 1000 rpm and welding speed of 60 mm/min. AA2014 was placed on the AS, while AA7075 was placed on the RS. FSW tool was fabricated from H13 tool material, and the tool was subjected to a heat treatment cycle to achieve specific

Table 2 — Mechanical properties of BMs

Alloy	Mechanical Properties		
	Ultimate Tensile Strength (MPa)	Elongation (%)	Hardness (Hv)
AA2014-T6	469.31 ± 3.12	7.82 ± 0.12	156.43 ± 3.15
AA7075-T6	553.64 ± 6.08	9.38 ± 1.98	173.29 ± 5.02
AA2014-O	173.85 ± 1.77	23.38 ± 0.18	59.5 ± 2.58
AA7075-O	208.50 ± 2.12	21.97 ± 0.58	68.5 ± 0.82

Table 1 — Chemical composition of BM AA2014 and AA7075

Alloy	Chemical Composition (Wt %)							
	Al	Cu	Zn	Mg	Mn	Si	Fe	Cr
AA2014	Bal.	4.71	-	0.25	0.86	0.52	0.37	-
AA7075	Bal.	1.56	6.25	2.26	-	-	0.32	0.22

hardness. The tool was heated to 1050 °C and soaked for 30 minutes. It was then cooled in ambient air to 50 °C and then again heated to 550 °C for 2 hours, followed by air-cooling¹⁹. FSW's tool had a 6° concave shoulder of 20 mm diameter and a threaded cylindrical pin of 6 mm diameter and 5.7 mm length.

2.4 Specimen preparation

After FSW, the developed welds were visually inspected for surface defects, and specimens for microstructural and mechanical characterization were then prepared by sectioning perpendicular to the welding direction. Samples were then polished as per standard metallographic practices using different emery papers to remove cutting marks and scratches from the surface. Mirror-finish surfaces were obtained by polishing with blazer and velvet cloth with 1 µm alumina powder. The polished samples were etched with Keller's solution (3 ml of HNO₃, 6 ml of HCl, 6 ml of HF, and 150 ml of water). After etching, samples were thoroughly washed and dried using an air drier. Microstructures were analyzed using an optical microscope (Make: Leica; Model DMI 500), and the microhardness was measured on the transverse weld section using Vickers microhardness tester (Make: UHL; Model: VMHT). A load of 1 N was applied for the 30s to make an indentation.

The transverse tensile specimens were prepared using a wire electric discharge machine according to the ASTM-E08M standard. Specimen width and gauge lengths were 6 mm and 25 mm respectively. Tensile tests were carried out on a computerized universal testing machine (Make: Tinius Olsen; Load Capacity: 50 KN) with a 1 mm/min crosshead speed. At least three tests were performed in each condition, and average results were reported for discussion. It is general practice to compare dissimilar welds'

properties with low strength BM, as failure occurs from low strength BM's region. Therefore, in this work, welds properties were compared with the strength or hardness of weak material of the dissimilar weld's combination. After tensile testing, the fracture surface of broken specimens was analyzed using Scanning Electron Microscope (Make: ZEISS; Model: SMT) to study the mode of fracture.

3 Results and Discussion

3.1 Microstructure

The microstructure of as received BMs (AA2014-T6 and AA7075-T6) is shown in Fig. 1. The AA2014 depicted less elongated and wider grains than the AA7075. The average grain size of AA2014 was 62 µm ± 34.57 µm length and 19 µm ± 12.67 µm width whereas that of AA7075 was 100 µm ± 64 µm length and 12 µm ± 5.73 µm width. The average aspect ratio of AA2014 was 3.26, whereas AA7075 was 8.33.

The SZ microstructure of AS and RS of welded joints in all four combinations of BMs are shown in Fig. 2. Irrespective of temper condition and their combination and side of the weld, the SZ exhibited fine dynamically recrystallized grains. The friction between the tool and the BM surface generated heat and softened the BM, and the material flowed from AS to RS with a rotating tool's stirring. Consolidation of the material at the trailing side of the tool forms a monolithic joint in solid-state. Severe plastic deformation produced by the rotating tool leads to continuous dynamic recrystallization of BM's coarse grains, resulting in grain refinement to form the equiaxed grain at the SZ.

After tool passing, the high temperature generated helps static grain growth and dissolution of precipitate

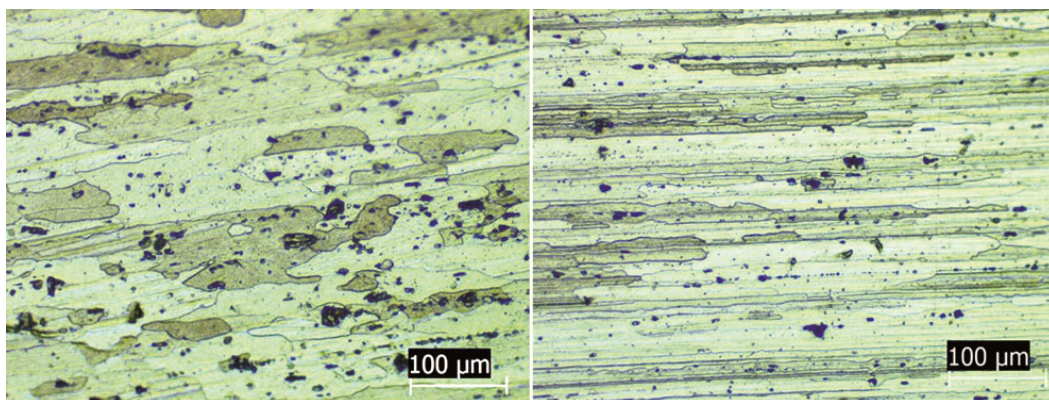


Fig. 1 — Microstructure of BM (a) AA2014-T6, and (b) AA7075-T6.

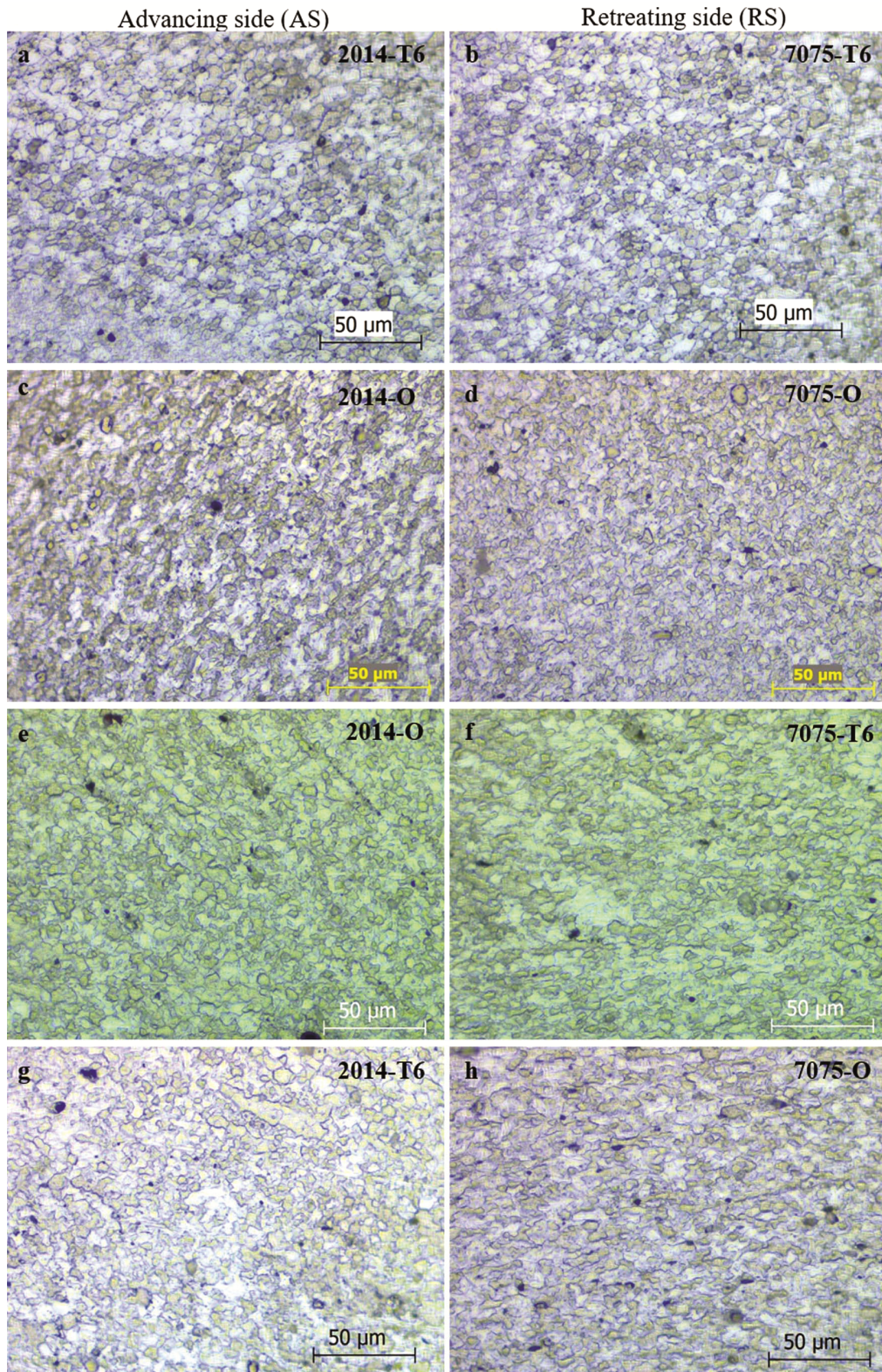


Fig. 2 — The microstructure of AS and RS of SZ in (i) 2O-7T6 (a and b), (ii) 2T6-7O(c and d), (iii) 2O-7O (e and f), and (iv) 2T6-7T6 (g and h).

or constituent particles present in the BM. Precipitate and constituent particles were dissolved in SZ, as shown in Fig. 2. It could be attributed to the high temperature generated at the SZ that exceeds the constituent particles' dissolution temperature. Variation of grain size on both sides of SZ (AS and RS) is presented in Table 3. The size of recrystallized grains was smaller on the RS of the weld. Grain growth depends on the degree of mechanical deformation, peak temperature, and exposure time to welded joints. As the welding parameter was constant for all the joints thus, the exposure time was constant. Still, the temperature generation and degree of mechanical deformation during welding depend on the respective BM's mechanical properties. AA7075 had higher flow strength than AA2014 due to the higher strength of AA7075.

The temperature generation on the RS was lower than the AS. A slip of material occurs at the RS, whereas material sticking occurs on AS, resulting in high frictional heating. Therefore, the grain size variation on both sides of SZ was observed. Moreover, BM temper and their combination influenced the shape of recrystallized grains, as evident from Fig. 2. Grains seem to be spherical in SZ of 2O-7T6 weld Fig. 2 (a and b), whereas angular grains can be observed easily for other welds Fig. 2 (c - h). Some large regions where grain boundaries couldn't completely form Fig. 2 (f and g) can also be seen.

Joint combination	Stir zone	
	AS (AA2014)	RS (AA7075)
2O-7T6	6.18 ± 2.00	5.89 ± 1.83
2T6-7O	6.79 ± 2.04	6.42 ± 1.99
2O-7O	6.64 ± 2.29	5.88 ± 2.39
2T6-7T6	7.72 ± 2.45	6.66 ± 2.74

Figure 3 shows the onion ring formed at the SZ in which intercalated structure consists of an alternate lamellar layer of both the BM because of complex solid state material flow²⁰. The onion rings were observed only in SZ of 2T6-7T6 and 2O-7O welded joints. The bright color band is solid solution rich in Cu i.e. AA2014, while the dark color band is solid solution rich in Zn i.e. AA7075 material, which could be distinguished due to the different etching responses of both the material. The spacing between these rings was more for 2T6-7T6 weld than 2O-7O welds. In the former weld's case, such rings' shape was crescent moon shape and confined to a small region, whereas later weld rings were concentric and larger. The formation of onion rings could be attributed to the flow of material with limited flowability in semi-circular batches by rotating and traversing tools. Onion rings displayed different profiles, possibly due to varying material flowability dependent on Base Metal (BM) type and temper, i.e., flow stress²¹.

3.2 Microhardness

Microhardness variation along the mid thickness of a transverse cross-section of welded joints is presented in Fig. 4 BM temper and their combination influenced the weld microhardness profiles significantly. In general, a W-shaped hardness profile is obtained for welds made with BM in T6 temper, whereas a flat profile with the risen central region was observed for welds made with BM in O temper. The softening of weld in HAZ and SZ region due to coarsening and dissolution of precipitates resulted in a W-shaped hardness profile.²² As expected for other welds consisting of T6 and O temper of BMs, the hardness profile was the combination of previous welds profile, i.e., one hand up and the other down. The welds' SZ was strengthened when at least one BM was in annealed O temper and softened when

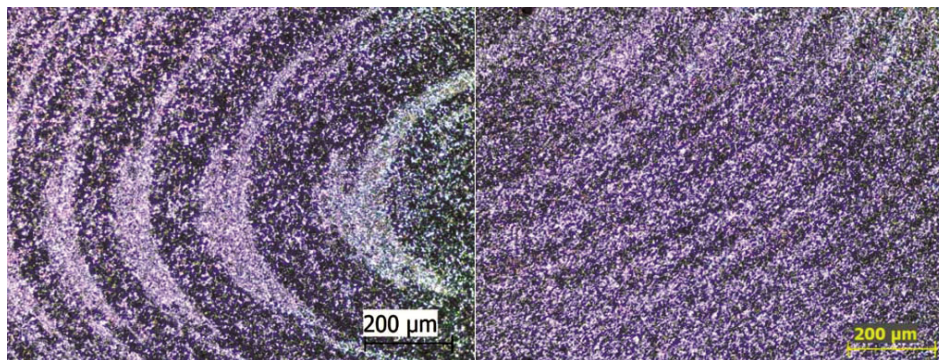


Fig. 3 — Onion ring formed in SZ of the welded joint (a) 2T6-7T6, and (b) 2O-7O.

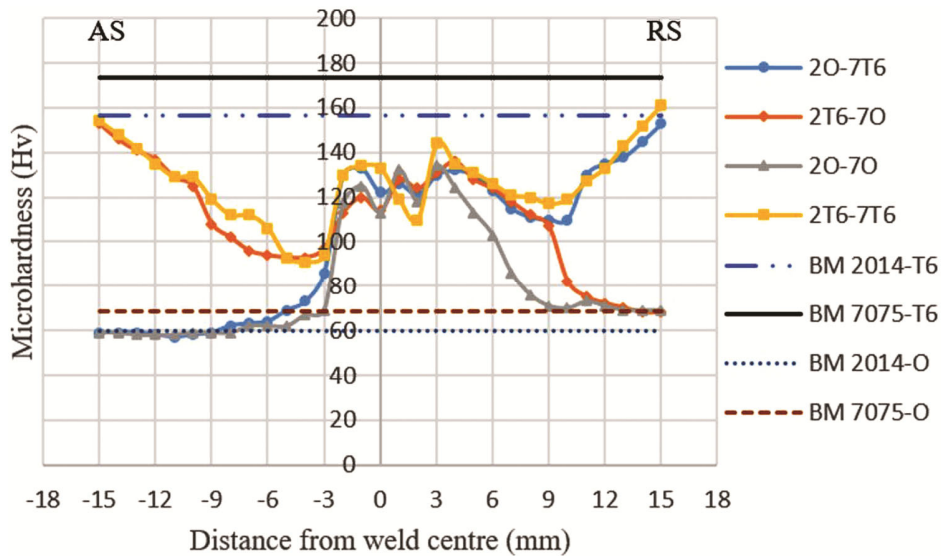


Fig. 4 — Influence of BM temper on weld microhardness along the cross-section.

both the BM were in T6 temper condition. The highest average microhardness of SZ was 123.43 Hv found for 2T6-7T6 welded joints.

On the other hand, the lowest average SZ microhardness of 115.43 Hv was found for 2O-7O-welded joints. The SZ hardness was much higher (approximately double) than O temper BM, significantly lower than T6 temper BM. The strengthening/softening of welds was observed mainly in the SZ, and the extent of the same was found to decrease moving away from the weld center. Therefore, hardness decreases when moving away from the SZ towards the HAZ side on both sides of the weld.

Also, the hardness in HAZ was affected significantly by the BM temper and their combinations. The HAZ hardness was lowest for 2T6-7T6 welds; an opposite trend was observed for 2O-7O welds. The hardness was seriously low in HAZ of welds involving at least one BM in T6 temper and high for welds with one BM in O temper. The decrease in HAZ hardness was more significant on the RS of the weld than AS, which could be attributed to softening in the welds' HAZ region because of thermal weld cycles.

In the T6 temper condition of BM, the microhardness value depends on the size and distribution of precipitate in the various weld zone. In the 2T6-7T6 weld, the microhardness value gradually decreased in RS (AA7075-T6) and AS (AA2014-T6) but gradually increased as it moved away from the SZ. It was due to the dissolution of the precipitate because of available higher temperatures sufficient to dissolve precipitates. The solid solution temperature

of AA7075 and AA2014 was 477°C and 507°C, respectively^{23, 24}. The extent of dissolution and coarsening of precipitate and grains seem to be more on RS than AS, resulting in more softening and loss of hardness in HAZ. The lowest hardness of 91 Hv was found at 4 mm from the welded line on the AS (AA2014-T6) of the weld. In 2O-7T6 and 2T6-7O weld, hardness value variation in annealed (2O and 7O) BM side followed a similar trend as in 2O-7O, and in T6 temper condition, BM alloy side (2T6 and 7T6) showed a similar trend as in 2T6-7T6 welded joint. The lowest value of microhardness in 2O-7T6 and 2T6-7O weld was observed in AS and RS of welded joints. The lowest hardness location in the 2O-7T6 and 2T6-7O welded joint was 11 mm from the welded line, and its value was 57 Hv and 75 Hv.

3.3 Tensile properties

UTS and PE of the various welded joints are presented in Fig. 5. The highest tensile strength among the welds was obtained for the 2T6-7T6 weld, followed by the 2T6-7O weld. Thus, when BM was welded in T6 temper, the resulting welds had higher tensile strength than welds in O temper. The tensile strength of 2T6-7T6 welds was 333 MPa and was comparable with the results of Sharma *et al.*²⁵, reported tensile strength of 330 MPa of dissimilar friction stir welds of 7039 and 2024 in T6 temper. On the other side, 2O-7T6 and 2O-7O welded joints' tensile strength were significantly lower than the above two joints with 2T6 on the AS. So, in welded joints, with O temper on the AS, the welded joints'

strength was almost similar to the low strength BM, i.e., AA2014-O, but the elongation of welded joints was substantially lower than the elongation of AA2014-O.

The PE of 12.88%, 11.66%, 13.41%, and 8.24% was obtained in welded joints of 2O-7T6, 2T6-7O, 2O-7O, and 2T6-7T6, respectively. Lower elongation of welded joint in O temper than the respective O temper BM may be attributed to higher hardness at the SZ because of which fracture occurred outside the weld zone where the lowest hardness exists.

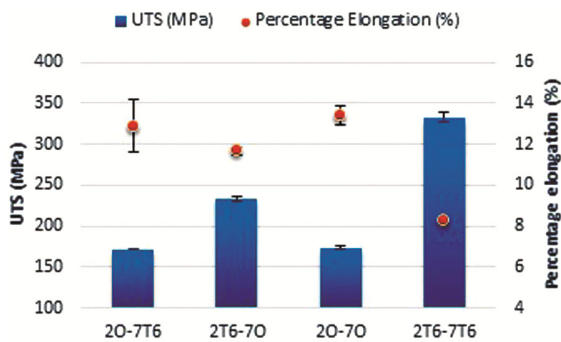


Fig.5 — Ultimate tensile strength and percentage elongation of 2O-7T6, 2T6-7O, 2O-7O, and 2T6-7T6

The dissimilar welds joint efficiency was calculated by taking the strength of the weakest BM of a particular combination into consideration and are presented in Table 4. In the investigated combinations, weak BM were different for welded joints due to different temper conditions of base metals. Therefore, for comparison an idea about the relative effect of tempers, joint and elongation performance were calculated with respect to AA2014-O and AA2014-T6. 2T6-7O joint shows the highest joint efficiency of 112.23% among the weld joints with O temper BM. In 2O-7T6 and 2O-7O joints, the joint efficiency was lowest for the 2O-7T6 joint though the difference was very marginal. The 2T6-7T6 joint fractured from the low hardness SZ region of the weld at a distance of 4.25 mm from the weld center and confirmed the observations of Fig. 4. In O tempered combination (2O-7T6, 2T6-7O, and 2O-7O) of welded joints, fracture occurred outside the welded SZ region from low strength BM as the joints' strength was more than or equal to the strength of O temper material (Table 5). Similar fracture location was obtained for welded friction stir joint of AA7039 in O temper which failed in BM region on RS far away from SZ²⁶.

Table 4 — Joint and elongation efficiency of welded joints with respect to (w.r.t.) weak metal of weld, AA2014-O, and AA2014-T6

Weld	Joint efficiency (UTS w.r.t. weak BM)	Joint Performance (UTS w.r.t. AA2014-O)	Joint Performance (UTS w.r.t. AA2014-T6)	Elongation efficiency (w.r.t. weak metal)	Elongation Performance (Elongation w.r.t. AA2014-O)	Elongation Performance (Elongation w.r.t. AA2014-T6)
2O-7T6	98.68	98.68	36.55	55.09	55.09	164.7
2T6-7O	112.23	134.6	49.86	53.07	49.87	149.1
2O-7O	99.68	99.68	36.93	57.36	57.36	171.5
2T6-7T6	70.96	191.54	70.96	105.37	35.24	105.37

Table 5 — Fracture location of the welded joints

Welded joint	AA7075	AA2014	Location (distance from weld center, side, and region)
2O-7T6			10.58 mm, AS, near the boundary of the weld region
2T6-7O			14.73 mm, RS, outside the weld region
2O-7O			13.46 mm, AS, outside the weld region
2T6-7T6			4.25 mm, AS, within weld region

3.4 Fracture

The surface morphology of the fractured tensile specimens of welded joints at low and high magnification is presented in Figs (6 and 7),

respectively. O temper combination of welded joints shows a significant necking effect before the fracture of the tensile specimen as the cross-section area was smaller than the original area of the fractured part, as

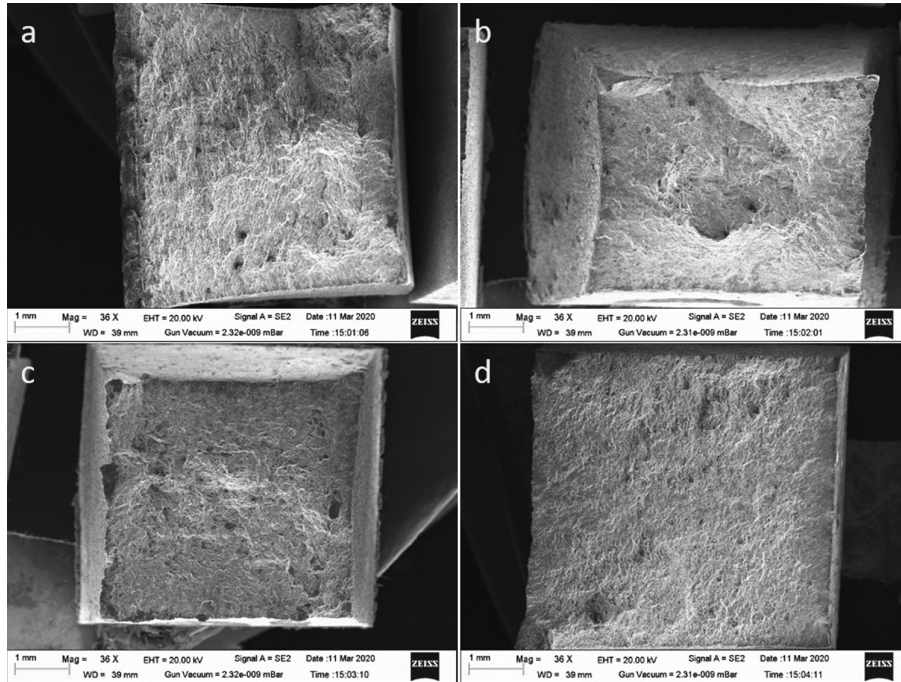


Fig. 6 — SEM images of the fracture surface of the tensile specimen at low magnification (a) 20-7T6, (b) 2T6-7O, (c) 20-7O, and (d) 2T6-7T6.

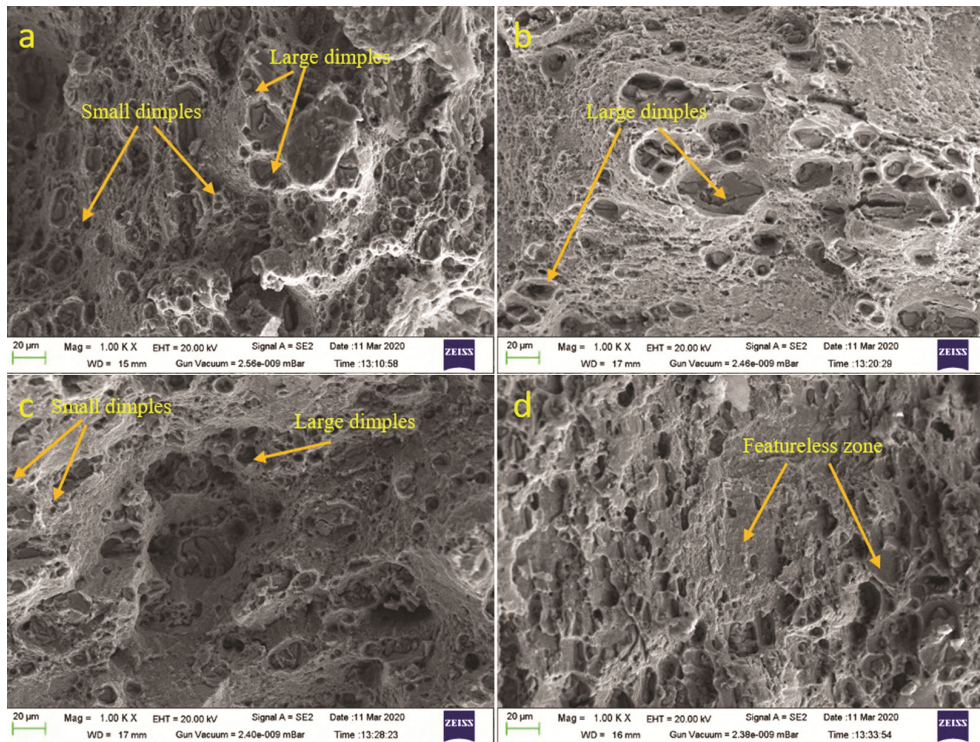


Fig. 7 — SEM images at a point on the fracture surface of welded joints (a) 20-7T6, (b) 2T6-7O, (c) 20-7O, and (d) 2T6-7T6.

evident from Fig. 6 (a - c). In contrast, the 2T6-7T6 joint did not show significant necking signs compared to formers. The 2O-7T6 specimen shows many fine and large dimples on the surface, leading to the highest ductility among all the joints Fig. 7 (a). Large and deep dimples were observed in 2T6-7O joints in Fig. 7(b) that yielded better ductility and high strength among the O temper weld. Small and large dimples appeared on the surface of 2O-7O Fig. 7 (c), which clearly showed the fracture's ductile mode. A rough and wavy surface was an indication of ductile fracture. In Fig. 7(d), many featureless zones were seen on the surfaces of 2T6-7T6 joints, which means that low plastic deformation resulted in the lowest ductility among all the joints. Small micro-cracks were also visible on the images of the fracture surface of 2T6-7O and 2T6-7T6 welds, as shown in Fig. 7 (b and d). The presence of microcracks on the fractured surface indicate decreased ductility. The fracture surface of 2T6-7T6 welds Fig. 7 (d) showed no deformation sign than other materials considered under study. Moreover, featureless regions on fracture surfaces suggest faster crack travel and reduced ductility of 2T6-7T6 welds.

4 Conclusion

The BM tempers influence the microstructure, hardness, tensile, and fracture properties of AA2014 and AA7075 friction stir welded joints. Specific conclusions from the study are given below:

- 1 The SZ microstructure was dominated by the BM placed on AS. SZ have equiaxed grains without constituent particles. Spherical grains were present in SZ of 2O-7T6, while others showed angular grains.
- 2 The hardness profile comprises characteristic softened and strengthened SZ and HAZ regions for welds made of BM in T6 and O temper. When weld consists of one BM in T6 temper and another in O temper, then hardness profile has the combination of former hardness profiles. The SZs and HAZs of welds made of BM in T6 temper exhibited hardness lower than BM, whereas a reverse trend was observed for O temper welds.
- 3 The weld joints' strength was either approximately equal or higher than the low strength BM of the combination and governed by BM on the weld. Despite severe softening in SZ and HAZ, the tensile strength of welds made of BM in T6 temper was approximately double than

that of welds consisting of at least one metal in O temper.

- 4 The welds failed from the BM region when at least one BM was in O temper and from the SZ when BM was in T6 temper, and all exhibited ductile mode of failure. Scarcity of dimples and presence of featureless zones on fracture surfaces of 2T6-7T6 weld was due to reduced ductility of weld metal.

Acknowledgment

The support provided by the Science and Engineering Research Board, India through Grant No. ECR/2016/001738 to carry out this research work is thankfully acknowledged.

References

- 1 Saravanan V, Banerjee N, Amuthakkannan R, & Rajakumar S, *Metallogr Microstruct Anal*, 4 (2015) 178.
- 2 Bahemmat P, Haghpanahi M, Givi M KB, & Seighalani K R, *Int J Adv Manuf Technol*, 59 (2012) 939.
- 3 Çam G, & İpekoğlu G, *Int J Adv Manuf Technol*, 91 (2017) 1851.
- 4 Kalembe-Rec I, Kopyściński M, Miara D, & Krasnowski K, *Int J Adv Manuf Technol*, 97 (2018) 2767.
- 5 Cavaliere P, Nobile R, Panella F W, & Squillace A, *Int J Mach Tools Manuf*, 46 (2006) 588.
- 6 Rajesh S, & Badheka V, *Mater Manuf Process*, 33 (2018) 156.
- 7 Ilangovan M, Boopathy S R, & Balasubramanian V, *Def Technol*, 11 (2015) 174.
- 8 Hu Z L, Wang X S, & Yuan S J, *Mater Charact*, 73 (2012) 114.
- 9 Chen Y, Liu H, & Feng J, *Mater Sci Eng A*, 420 (2006) 21.
- 10 Sharma C, Dwivedi D K, & Kumar P, *Mater Sci Eng A*, 620 (2015) 107.
- 11 Aydın H, Bayram A, Uğuz A, & Akay K S, *Mater Des*, 30 (2009) 2211.
- 12 Yan J, & Reynolds A P, *Sci Technol Weld Join*, 14 (2009) 282.
- 13 İpekoğlu G, Erim S, & Çam G, *Int J Adv Manuf Technol*, 70 (2014) 201.
- 14 Lin H, Wu Y, & Liu S, *Mater Charact*, 146 (2018) 159.
- 15 Chen J, Li S, Cong H, & Yin Z, *J Mater Eng Perform*, 28 (2019) 916.
- 16 Al-Dwairi A F, Abdelal E, & Rivero I, *Metallogr Microstruct Anal*, 9 (2020) 169.
- 17 İpekoğlu G & Çam G, *Metall Mater Trans A*, 45 (2014) 3074.
- 18 ASM Handbook Volume 4, Heat treating, ASM international, 1991.
- 19 Hasan M M, Ishak M, & Rejab M R M, *Int J Adv Manuf Technol*, 98 (2018) 2747.
- 20 Sharma C, & Upadhy V, *Engg Rev*, 41 (2021) 107.
- 21 Sharma C, Dwivedi D K, & Kumar P, *Mater Des*, 36 (2012) 379.
- 22 Sharma C, Dwivedi D K, & Kumar P, *Mater Des*, 43 (2013) 134.
- 23 Cole E G, Fehrenbacher A, Duffie N A, Zinn M R, Pfefferkorn F E, & Ferrier N J, *Int J Adv Manuf Technol*, 71 (2014) 643.
- 24 Jonckheere C, Meester B D, Denquin A, & Simar A, *J Mater Process Technol*, 213 (2013) 826.
- 25 Sharma C, Upadhy V, & Narwariya BS, *Mater Res Express*, 6 (2019) 026524.
- 26 Sharma C, Dwivedi D K, & Kumar P, *Engg Rev*, 35 (2015) 267.